Published in final edited form as:

Mol Nutr Food Res. 2020 August ; 64(15): e2000341. doi:10.1002/mnfr.202000341.

Targeting the liver-brain axis with hop-derived flavonoids improves lipid metabolism and cognitive performance in mice

Ines L. Paraiso[a,b,*], **Johana S. Revel**[a,b,c,*], **Jaewoo Choi**[a], **Cristobal L. Miranda**[a,b], **Parnian Lak**[a,b,c], **Chrissa Kioussi**[b], **Gerd Bobe**[a,d], **Adrian F. Gombart**[a,e], **Jacob Raber**[b,f], **Claudia S. Maier**[c], **Jan F. Stevens**[a,b]

[a]Linus Pauling Institute, Oregon State University, Corvallis, OR, 97331, USA

[b]Department of Pharmaceutical Sciences, Oregon State University, Corvallis, OR, 97331, USA

[c]Department of Chemistry, Oregon State University, Corvallis, OR, 97331, USA

[d]Department of Animal & Rangeland Sciences, Oregon State University, Corvallis, OR, 97331, USA

[e]Department of Biochemistry & Biophysics, Oregon State University, Corvallis, OR, 97331, USA

[f]Department of Behavioral Neuroscience, Neurology, and Radiation Medicine, Division of Neuroscience, Oregon National Primate Research Center, Oregon Health & Science University, Portland, OR, 97239, USA

Abstract

Scope: Sphingolipids including ceramides are implicated in the pathogenesis of obesity and insulin resistance. Correspondingly, inhibition of pro-inflammatory and neurotoxic ceramide accumulation prevents obesity-mediated insulin resistance and cognitive impairment. Increasing evidence suggests the farnesoid X receptor (FXR) is involved in ceramide metabolism, as bile acid-FXR crosstalk controls ceramide levels along the gut-liver axis. We previously reported that FXR agonist xanthohumol (XN), the principal prenylated flavonoid in hops (*Humulus lupulus*), and its hydrogenated derivatives, α,β-dihydroxanthohumol (DXN) and tetrahydroxanthohumol (TXN), ameliorated obesity-mediated insulin resistance and cognitive impairment in mice fed a high-fat diet (HFD).

Methods and results: To better understand how the flavonoids improved both, we analyzed lipid and bile acid profiles in the liver, measured sphingolipid relative abundance in the hippocampus, and linked them to metabolic and neurocognitive performance. XN, DXN and TXN (30mg/kg BW/day) decreased ceramide content in liver and hippocampus; the latter was linked to

Correspondence and requests for materials should be addressed to J.F.S. fred.stevens@oregonstate.edu.

*These authors have contributed equally to this article

Authors contributions

I.L.P., J.S.R., J.C., P.L., J.R., J.F.S. designed the experiments. I.L.P., J.S.R., J.C., P.L. performed the experiments. I.L.P., G.B., J.S.R., J.C., J.R. analyzed the data and performed statistical analyses. I.L.P., J.S.R., J.C., C.L.M., P.L., C.K., G.B., A.F.G., J.R., C.S.M., J.F.S. provided scientific, technical and material support, wrote and reviewed the manuscript.

Conflict of interest

The authors declare no conflict of interest.

Supporting information

Supporting Information is available from the Wiley Online Library or from the author.

improvements in spatial learning and memory. In addition, XN, DXN and TXN decreased hepatic cholesterol content by enhancing *de novo* synthesis of bile acids.

Conclusion: These observations suggest that XN, DXN and TXN may alleviate obesity-induced metabolic and neurocognitive impairments by targeting the liver-brain axis.

Graphical Abstract

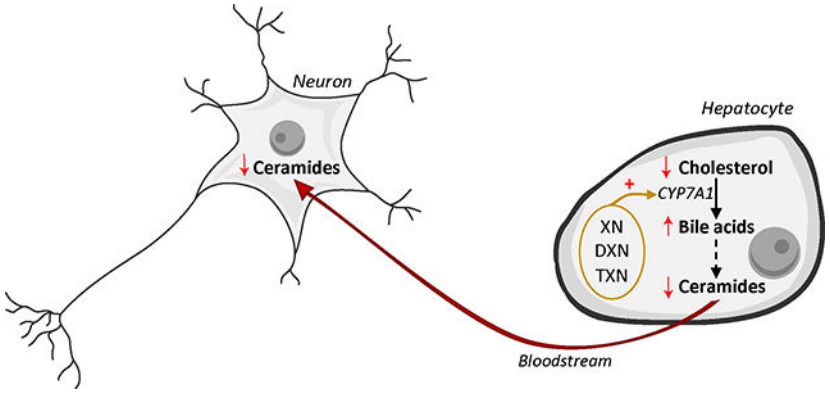

Keywords

Bile acids; ceramide; cholesterol; obesity

1. Introduction

Metabolic syndrome (MetS) is a cluster of conditions including impaired insulin sensitivity and hyperglycemia, abdominal obesity, hypertension, and dyslipidemia with elevated blood triglycerides (TG), elevated LDL-cholesterol, and with depressed HDL-cholesterol, abdominal obesity and hypertension [1, 2]. Feeding rodents a high-fat diet (HFD) is a well-established method to generate a preclinical model of metabolic disorders [3]. Mice fed a HFD exhibit an increase in body weight, visceral fat, dysregulation in plasma metabolic parameters (elevated fasting plasma glucose, fasting plasma insulin and HOMA-IR index) and increased hepatic TG and cholesterol [3–5]. Obesity affects a large number of biochemical processes and excess adiposity antagonizes insulin action in peripheral tissues by various mechanisms. First, obesity triggers a chronic inflammatory state, in which adipose tissue releases increased amounts of non-esterified fatty acids, glycerol, adipocyte-derived hormones, pro-inflammatory cytokines and other factors that are involved in the development of insulin resistance and type 2 diabetes [6–8]. Second, in obese individuals, the increase in intracellular content of fatty acid metabolites, including diglycerides (DG) and ceramides, activates a serine/threonine kinase cascade leading to phosphorylation of insulin receptor substrates, which in turn, attenuates the ability of insulin to activate the PI3K (phosphoinositide-3-kinase) pathway [9, 10]. Consequently, glucose transport and other downstream of insulin receptor signaling cascades are compromised. Additionally, obesity and type 2 diabetes are associated with brain mitochondrial dysfunction and brain insulin resistance as indicated by impairment of insulin-induced long-term depression in the hippocampal areas [11–15].

Ceramides may serve as key intermediates linking saturated fat to inhibition of insulin signaling. Saturated fatty acids induce the formation of ceramides and glucosylceramides [16, 17], and elevated ceramide levels have been linked to obesity, insulin resistance [18, 19] and mitochondrial dysfunction [18, 20]. Moreover, ceramides are lipid soluble and readily cross the blood-brain barrier [21]. Therefore, peripheral insulin resistance and the associated hepatic and adipocyte production of neurotoxic ceramides in obesity could account for the co-occurrences of cognitive impairment and neurodegeneration [22, 23]. As a result, inhibition of ceramide synthesis ameliorates HFD-induced obesity and insulin resistance [16, 24]. Pharmacological strategies aimed at modulating ceramide levels have beneficial effects on the complications of metabolic diseases [16, 25].

Intestinal ceramide synthesis is under the control of the farnesoid X receptor (FXR) [20, 25], a nuclear receptor with a central role in glucose, lipid and bile acid homeostasis. Biological modulators of FXR include bile acids (BAs), a group of hydroxylated steroids synthesized in the liver from cholesterol, and secreted into the intestine, where they emulsify dietary lipids [26]. BAs are no longer considered simple surfactants that increase absorption of hydrophobic nutrients but are known signaling molecules that modulate the activity of FXR and other nuclear receptors in multiple organs [27–30]. As a result, bile acid receptor modulators are also attractive alternatives treatments for MetS.

Xanthohumol (XN), the principal prenylated flavonoid found in hops (*Humulus lupulus*), exerts anti-obesity effects in HFD-fed animals [31–33]. Our previous studies show that treating HFD-fed C57BL/6J mice orally with XN (30 or 60 mg/kg/day) attenuates metabolic aberrations associated of MetS, including elevated plasma levels of low-density lipoprotein-cholesterol (LDL-c), LDL receptor-degrading enzyme proprotein convertase subtilisin/kexin type 9 (PCSK9), interleukin-6 (IL-6), leptin and HOMA-IR compared with vehicle/HFD controls [33, 34]. Due to an α,β-unsaturated ketone in its chemical structure, XN can spontaneously form a stable isomer, isoxanthohumol (IX), the biological precursor to the potent phytoestrogen, 8-prenylnaringenin (8PN) [35, 36]. As a result, the use of XN in dietary supplements raises concerns because of the potential estrogenic side effects. Because 8PN itself also attenuates body weight gain, and improves metabolic parameters associated with obesity, the biological effects of XN might, in part, be mediated by the formation of 8PN [37]. To distinguish between the metabolic and pro-estrogenic properties of XN, we examined two hydrogenated derivatives of XN, *i.e.*, α,β-dihydroxanthohumol (DXN), a product of XN reductive metabolism by intestinal bacteria [38], and tetrahydroxanthohumol (TXN), a synthetic derivative of XN. DXN and TXN cannot be converted into 8PN and have no intrinsic estrogenic activity but retain the metabolic properties of XN [34]. We induced metabolic disorders by feeding young adult C57BL/6J mice a HFD supplemented with XN, DXN or TXN, and evaluated the pharmacological and cognitive properties of these flavonoids and reported them as attractive treatment options to mitigate MetS and cognitive impairments associated with obesity [34]. In the current study, we performed a global lipidomic and bile acid analysis of liver from the same mice treated with XN, DXN or TXN to determine their effect on hepatic lipid and bile acid composition. In order to identify the mechanisms associated with the improved hippocampus-dependent learning and memory observed in our previous study [34], we also analyzed hippocampal sphingolipid content in these mice.

2. Experimental Section

2.1. Animal study design

All animal experiments were performed in accordance with institutional and National Health and Medical Research Council guidelines. The experimental protocol (protocol # 4501) was approved by the Institutional Animal Care and Use Committee at Oregon State University and the studies were carried out in accordance with the approved protocol. The animal study design was described previously and experimental parameters such as food intake, body weight and cognitive function were reported in the study by Miranda et al. [34]. Nine-week old male C57BL/6J mice were obtained from The Jackson Laboratory (Bar Harbor, ME, USA) and housed individually under a 12–12-hr light-dark cycle. They were assigned randomly to four groups of 12 mice each: one group (control) was fed a HFD (Dyets Inc., Bethlehem, PA, USA), and the other three groups were fed the HFD containing XN, DXN, or TXN (purity >99%) from Hopsteiner Inc. (New York, NY, USA). The mouse diets were formulated to deliver a dose of 30 mg test compound per kg body weight per day, the test compounds were first dissolved in OPT (oleic acid:propylene glycol:Tween 80, 0.9:1:1 by weight) before mixing with the diet at a concentration of 0.033%. Calorie intake from HFD was 60% kcal from fat, 20% kcal from carbohydrate, and 20% kcal from protein. Long-term spatial memory retention was tested in a 60-second probe trial and time spent in target quadrant compared to non-target quadrants was analyzed as described [34]. At the end of 13 weeks of feeding, the mice were euthanized, and hippocampus as well as liver were dissected for analyses.

2.2. Brain and liver lipidomics

Liver and brain lipids were extracted using one phase solvent system (500 μL, 25:10:65 v/v/v system of methylene chloride: isopropanol: methanol, with 50 μg/mL butylated hydroxytoluene [BHT]) with some modification [39]. Liver samples (approximately 50 mg, n = 9–12 per group) were homogenized with 0.5 mm zirconium oxide beads (Next Advance Inc., Troy, NY, USA) using a counter-top bullet blender for 3 min, incubated at −20°C for one hour, and the homogenates were centrifuged at 4°C at 15,000 × g for 10 min. The same extract preparation method was used for hippocampal tissues from approximately 10 mg of material (n = 9–12 per group). From each extract, a 40 μL aliquot from the supernatant was transferred to an autosampler vial, and, 155 μL of extraction solvent and 5 μL of Splash® Lipidomix® Mass Spec Standard (Avanti Polar Lipids, Alabaster, AL, USA) were added. Samples were stored at −80°C until further analysis. LC and MS conditions were developed by our group and described previously [40].

2.3. Liver bile acids analysis

Approximately 50 mg of liver samples (n = 9–12 per group) were extracted with 6 μL/mg of cold ethanol:methanol (1:1, v/v) and 0.4 μmol of deuterated chenodeoxycholic acid (CDCA-d4) per mg of tissue. Samples were homogenized with 0.5 mm zirconium oxide beads at 6.5k rpm, 2 × 45 seconds and then centrifuged for 10 minutes at 10k rpm at 4°C. The supernatant was transferred to a clean 1.5 mL microcentrifuge tube using a gel-loading tip and filtered into a mass spectrometry vial using a PTFE syringe filter. A quality control (QC) sample was prepared by pooling 5μL of each fecal sample to monitor suitability,

repeatability and stability of the LC-MS system. Samples were stored at −80°C before analysis. LC and MS conditions were as described previously [41]. Peak alignment, feature extraction and normalization were performed using Progenesis QI (Waters, Milford, MA, USA). Bile acids were identified by matching their retention time, isotopic pattern, accurate mass of the $[M-H]^-$ ion and fragmentation pattern with those of authentic commercial standards obtained from Sigma-Aldrich (St Louis, MO, USA). The area of the base peak extracted ion chromatogram was selected for relative quantitation.

2.4. Cell cultures

Human HepG2 liver cancer cells (Signosis, Santa Clara, CA, USA) were cultured in 100 mm × 15 mm petri dishes using DMEM (Corning, Corning, NY, USA) supplemented with 10% fetal bovine serum. Prior to treatment, HepG2 cells were plated in 6-well plates at a density of 5.10^4 cells per well. After 24h of incubation at 37°C in a 5% CO_2 atmosphere, fresh medium containing 10 μM of CDCA (Sigma-Aldrich, St Louis, MO, USA), XN, DXN, TXN or vehicle (DMSO) was added to the cells. After 48h of incubation, RNA was isolated (Qiagen, Hilden, Germany) and stored at −80°C until further processed.

2.5. Gene expression analysis

For real-time quantitative polymerase chain reaction (qPCR), RNA samples from mice liver samples (n = 4–5 per group) and HepG2 cell cultures (n = 3 per group) were reverse-transcribed using the High-Capacity cDNA Reverse Transcription Kit (Applied Biosystems, Waltham, MA, USA). Universal SYBR® Green Supermix (Bio-Rad, Hercules, CA, USA) was used following the manufacturer's protocol and amplifications were performed using the ABI Prism 7300 Real-Time PCR System (Applied Biosystems, Waltham, MA, USA). Each sample was tested in triplicate. Gene expression was normalized to levels of Polymerase-II. Relative gene expression was calculated using the ddCt method. All primers are listed in Table S1.

2.6. Statistical analysis

Boxplots and bar plots are represented as mean ± SEM. Heatmaps were made using MetaboAnalyst v.4.0.; for a given feature, each cell represents the average of individual values from the same group. Statistical analyses were performed with the GraphPad Prism Software v.8.0 using one-way ANOVA with diet as fixed effect. The a priori comparisons were all three flavonoid groups combined vs. control and each flavonoid group vs. control. Due to the not normal distribution of the bile acids, the non-parametric Wilcoxon rank-sum test was used for the bile acid data. The significances were marked in tables and graphs with an asterisk: *$p < 0.05$, **$p < 0.01$, ***$p < 0.001$, ****$p < 0.0001$. To evaluate the association between metabolic and neurocognitive performance with liver and hippocampal lipid profile, respectively, parametric Pearson correlation coefficients and nonparametric Spearman's rank-order correlation coefficients were calculated. The same correlation coefficient was used to determine whether hippocampal sphingolipid profile changes followed liver lipid profile changes.

3. Results

3.1. XN, DXN and TXN displayed anti-hyperlipidemic properties in HFD-fed mice

We performed global lipidomic profiling of liver tissues from control mice fed a HFD and treated mice fed a HFD containing XN, DXN or TXN. Within the features detected by UPLC-ESI-QTOF-MS operated in the negative and positive ionization modes, a total of 148 lipid species covering 4 lipid classes and 15 lipid sub-classes were annotated and quantified by normalization of their chromatographic peak areas over the structurally closest internal standards. Partial least-squares discriminant analysis (PLS-DA) modeling of the hepatic lipid profile revealed distinct separation between control and treatment groups (Fig.1A). Hierarchical clustering showed 9 out of the 15 measured lipid sub-classes clustered in their response to the flavonoids and were gradually lower from XN to DXN and, to TXN, compared with the control group. This cluster included lysophosphatidylethanolamine (LPE), lysophosphatidylcholine (LPC), lysophosphatidylinositol (LPI), cholesterol (Chol), cholesterol esters (CE), ceramides (Cer), sphinganines (Spha), sphingosines (Spho) and triglycerides (TG) (Fig.1B). Of the remaining 6 lipid sub-classes, diglycerides (DG) and phosphatidylserine (PS) clustered with higher values in the treatment groups than the control group.

In our analysis, glycerophospholipids were the most abundant class of lipids in the liver. While flavonoid treatments did not affect the relative abundance of phosphatidylethanolamine (PE), phosphatidylcholine (PC) and phosphatidylinositol (PI) (Fig.S1A–C), their lyso-derivatives, *i.e.*, LPE, LPC and LPI were significantly decreased in at least two of the flavonoid groups. LPE ($p = 0.0004$) was decreased by 32% and 40%, while LPC ($p = 0.0003$) was decreased by 25% and 33% in DXN and TXN-treated mice respectively (Fig.1C–D). LPI ($p < 0.0001$) was decreased by 35%, 52% and 50% in XN, DXN and TXN-treated mice respectively (Fig.1E). As a result, the ratio of lyso-derivatives to PE, PC and PI was reduced in the liver of flavonoid-treated mice ($p < 0.0001$). In contrast to lipids from the same class, phosphatidylserine (PS) was increased by at least 55% in the treatment groups ($p = 0.0003$; Fig.S1D).

Sterols, the second most abundant class of lipids identified in the liver were decreased by 15%, 23% and 40% with XN, DXN and TXN treatment, respectively ($p = 0.01$; Fig.S1E). Within that class, XN, DXN and TXN lowered relative abundance of both CE ($p = 0.02$) and cholesterol ($p < 0.0001$) in the liver of treated HFD-fed mice (Fig.1F–G). In the glycerolipids class, TG was significantly decreased in DXN- and TXN-treated mice by 18% and 27%, respectively ($p = 0.007$; Fig.1H), whereas relative abundance of DG was increased ($p = 0.02$). As a result, the TG/DG ratio was significantly lower in the XN-, DXN- and TXN-treated mice than control mice ($p = 0.001$; Fig.S1F). Sphingolipids including sphingomyelin (SM) precursors, *i.e.*, ceramides ($p < 0.0001$), Spha ($p = 0.0004$) and Spho ($p < 0.0001$) were decreased in the liver of flavonoid-treated mice. The relative abundance of ceramides was lowered by 22%, 38% and 46% in XN, DXN and TXN groups, respectively, while SM levels were not affected by treatment ($p = 0.32$; Fig.1I–J).

In summary, XN and its hydrogenated derivatives displayed anti-hyperlipidemic properties in HFD-fed mice by decreasing hepatic TG content, hepatic cholesterol, and by depleting the pool of lysophospholipids and SM precursors.

3.2. XN, DXN and TXN decreased hippocampal ceramides in HFD-fed mice

To determine if the anti-hyperlipidemic effects of XN and derivatives in the liver were associated with lipid changes in the brain, we measured hippocampal sphingolipid levels in both control and flavonoid-treated mice. A total of 12 sphingolipid species including ceramides and SM were annotated (Fig.S2A). In our analysis of ceramides in the hippocampus, normalization using internal standards alone was unable to correct for the variations resulting from handling very small amounts of extracted material. As ceramides can be derived from SM catabolism by sphingomyelinases or through degradation of complex sphingolipids in late endosomes and lysosomes [22, 42–44] (Fig.2A), we performed an additional intra-sample normalization using SM contents to correct for these variations. Ultimately, each sample was normalized to the weight of extracted material and internal standard, and each of the identified ceramide features was further normalized to the corresponding SM (SM with isomeric side chain) levels (Fig.2B). The total amounts of ceramides in the hippocampus were significantly decreased by 15% in XN and DXN-treated mice, and by 21% in TXN-treated mice in comparison to the control HFD-fed mice ($p = 0.002$; Fig.2C). The changes in the treatment groups were significant for individual ceramides C18 ($p = 0.04$) and C22:1 ($p = 0.004$) but the decrease in total hippocampal ceramides was driven primarily by the most abundant (75–80%) ceramide fraction C22:1.

Mice fed a HFD supplemented with XN, DXN, or TXN exhibited spatial memory retention in the probe trial and spent more time in the target quadrant, which contained the hidden platform during the training trials, than any other quadrant, while mice fed only a HFD did not [34]. Therefore, we assessed whether total amounts and individual ceramides in the hippocampus were associated with cognitive performance, as measured by the percent time spent in the target quadrant during the water maze probe trial. The total amounts of ceramides in the hippocampus were significantly negatively correlated with the percent time spent in the target quadrant in the water maze probe trial ($r = -0.402$, $p = 0.006$) (Fig.2D). Additionally, there was a significant negative correlation between hippocampal C22:1 ceramide and percent time spent in the target quadrant in the water maze probe trial ($r = -0.368$, $p = 0.012$) (Fig.S2B), but this was not seen for other ceramide species. We observed a significant positive correlation between total ceramide levels in the hippocampus and in the liver ($r = 0.309$, $p = 0.049$) (Fig.2E), which effectively linked the relative abundance of ceramides in the brain to cognitive performance as well as relative abundance of ceramides in the liver.

3.3. XN, DXN and TXN induced expression of genes involved in ceramide metabolism in HFD-fed mice

We measured relative gene expression of genes involved in synthesis and degradation of ceramides in the liver of HFD-fed mice upon treatment with XN, DXN and TXN. Gene expression profiles were different in DXN and TXN-treated than XN-treated mice. While XN increased the expression of 10 out of 13 measured genes, including sphingolipid delta

desaturase 2 (*Degs2*), ceramide synthase (*Cers2*, *Cers4*, *Cers5*, *Cers6*) and sphingomyelinase (*Smpd1*, *Smpd3*, *Smpd4*) genes involved in ceramide synthesis, as well as sphingomyelin synthase genes (*Sgms1*, *Sgms2*) involved in ceramide catabolism (Table 1). In the liver, DXN and TXN both induced the expression of serine palmitoyl transferase gene (*Sptlc1*) and *Smpd4* (Table 1). In summary, expression of genes involved in ceramide metabolism was differentially induced by XN compared to DXN and TXN.

3.4. XN, DXN and TXN increased hepatic primary BAs in HFD-fed mice

To determine the impact of XN and its derivatives on hepatic bile acid pool size and composition, liver BAs were extracted and analyzed for total BAs as well as individual bile acid species. Using standards, 11 individual unconjugated and taurine conjugated BAs were identified by UPLC-MS (Fig.3A). Mice treated with XN and its derivatives displayed no significant changes in total liver BAs relative abundance compared to the control (Fig.S3A), however, total BAs were increased when all 3 flavonoid groups were combined ($p = 0.04$). The changes were driven primarily by an increase in primary unconjugated BAs, as XN, DXN and TXN treatments were respectively associated with 73%, 78% and 169% increase in relative abundance of primary unconjugated BAs in the liver (Fig.3B). Significant or near significant increases ($p < 0.10$) were observed for the 3 identified primary unconjugated BAs, *i.e.*, cholic acid (CA; $p = 0.10$), α-muricholic acid (α- MCA; $p = 0.001$) and β-muricholic acid (β-MCA; $p = 0.01$) (Fig.3C–E). Similarly, all 3 identified primary taurine conjugated BAs, *i.e.*, taurocholic acid (TCA; $p = 0.04$), taurochenodeoxycholic acid (TCDCA; $p = 0.06$), and tauro-α-muricholic acid (T-α-MCA; $p = 0.03$) were significantly or near significantly increased (Fig.S3B–D). In contrast, the secondary bile acid ω-MCA was decreased by 59% and 53% in DXN and TXN treatment groups ($p = 0.02$; Fig.S3E), while taurine conjugated secondary BAs T-ω-MCA ($p = 0.68$) and taurodeoxycholic acid (TDCA; $p = 0.44$) were not altered. Relative abundance of primary unconjugated BAs negatively correlated with CE in the liver ($r = 0.382$, $p = 0.011$) (Fig.3F), linking the increased primary BAs to decreased sterol contents in the liver.

3.5. XN, DXN and TXN induced FXR target genes stronger than CDCA *in vitro*

To investigate the effect of XN and its derivatives on FXR target genes, we exposed human liver cancer cells (HepG2) to 10 μM of XN, DXN, TXN, or the FXR agonist CDCA and measured relative gene expression of 4 FXR-regulated genes. All 4 treatments significantly induced expression of the small heterodimer partner (*Shp*) gene, whereas *Cyp7a1* and bile salt export pump (*Bsep*) expression were increased only by the 3 flavonoids and the sterol regulatory element-binding protein 1c (*Srebp1c*) were increased only by TXN (Table 2). In summary, at 10 μM concentration, XN, DXN and TXN induced expression of FXR target genes in HepG2 cell lines; their effect stronger than for the known FXR agonist CDCA.

4. Discussion

Obesity and MetS are often associated with altered lipid homeostasis in the liver resulting in non-alcoholic fatty liver [45, 46], which is characterized by an accumulation of hepatic TG. Previous results have shown that hepatic TG concentrations are significantly reduced in XN-treated mice [33, 47]. Furthermore, we have reported a decrease in markers of

hepatotoxicity, reduced weight gain and improved glucose tolerance in mice treated with XN, DXN or TXN compared to the HFD control group [34]. In the current study, despite the decreasing trend in TG relative abundance in XN-treated mice, the difference compared to the control mice did not reach statistical significance. However, DXN and TXN significantly decreased hepatic TG in HFD-fed mice, which could be a result of the greater steady-state liver and plasma concentrations of DXN and TXN compared to XN [34]. The product/precursor ratio of TG over DG, revealed a significant decrease in the TG/DG ratio, suggesting a mitigation of the enzyme diacylglycerol acyl transferase (DGAT) activity by XN, DXN and TXN. This observation is in agreement with previous findings showing an inhibitory effect of XN on DGAT activity in rat microsomes [48] and with reports that DGAT knockdown ameliorates non-alcoholic fatty liver in obese mice [49, 50].

Circulating levels of lysophospholipids LPC, LPE, and LPI have been reported to decrease following a hypocaloric diet and weight loss [51] but there is limited understanding about the role of these lipid species in metabolic overload diseases and existing data are contradictive. For instance, a marked increase in plasma levels of LPC has been described in obesity [52, 53], while contradicting results have shown that HFD is associated with a decrease in hepatic LPC [54, 55]. In our study, improvement of MetS biomarkers was linked to a decrease in hepatic LPC, LPE and LPI. Interestingly, relative abundance of hepatic PS went against the general trend, as PS, a critical membrane phospholipid, was significantly increased in the treatment groups. In fact, reduced PS transfer to the mitochondria leads to endoplasmic reticulum stress, inflammation, TG accumulation in mice [56] and dietary PS improves cognitive function in animals and humans [57].

There is a consensus that ceramides serve as a putative intermediate linking excess in nutrients (*i.e.*, saturated fatty acids) to production of inflammatory cytokines (*e.g.*, TNF-α), and antagonism of insulin signaling [17, 18]. Cytotoxic ceramides originating from the periphery may mediate neurodegeneration and cognitive impairment [23, 58]. In fact, obesity-induced hippocampal insulin resistance is mediated through different metabolic changes, including increased ceramide levels leading to impaired brain insulin PI3K-Akt signaling [59] and neurodegeneration [22, 60–62]. Our study reveals a decrease in ceramides in the liver and hippocampus of XN-, DXN- and TXN-treated mice. In XN-treated mice, the decrease in hepatic ceramides was associated with an increase in mRNAs encoding enzymes involved in synthesis and degradation of ceramides, suggesting an accelerated turnover of ceramides in the liver. On the other hand, DXN and TXN increased gene expression of sphingomyelinases responsible for the synthesis of ceramides from SM, suggesting a differential mechanism of regulation of ceramide levels by the flavonoids. We report a correlation between decreased hepatic ceramides, decreased hippocampal ceramides and enhanced spatial memory retention. This could explain the improvement in both hippocampus-dependent learning and memory as well as the improvement in peripheral metabolic impairments in treated mice [34]. Our results suggest the peripheral actions of XN, DXN and TXN partially mediate their effects on neurocognitive function, which is in agreement with multiple reports of a liver-brain axis connecting peripheral and neural insulin resistance [15, 22].

The link between insulin resistance, ceramides and BAs is nonlinear and, likely involves the nuclear receptor, FXR. FXR serves as a primary sensor of nutritional cues, translating stimuli into transcriptional programs [63] and regulates glucose and lipid metabolism by repressing the transcriptional activation of enzymes involved in gluconeogenesis, *de novo* lipogenesis and bile acid homeostasis [64, 65]. A bile acid–FXR signaling axis has been shown to control ceramide synthesis in the intestine, as inhibition of intestinal FXR results in the repression of pro-ceramide genes [25, 66]. Moreover, FXR agonism stimulates adiponectin secretion [67] and adiponectin receptor expression in hepatocytes [68]. The existence of an adiponectin–ceramidase connection driving the improvement of metabolic function has been proposed as adiponectin signaling was found to lower ceramide concentrations [69]. Therefore, it is reasonable to consider the bile acid–FXR–ceramide signaling axis as a tangible multi-organ pathway, which plays a role in the regulation of insulin signaling and metabolic disorders. However, whether activation of FXR is more beneficial than its inhibition for the treatment of metabolic diseases remains under investigation.

XN, DXN and TXN act as FXR agonists by activating FXR target genes in the liver of treated mice [41] and in cell culture. *Srebp1c* gene expression was increased in TXN-treated cells, which could be explained by post-translational regulation of the protein, as XN was found to decrease the mature form of hepatic SREBP1 by suppressing its processing [41, 70]. XN and TXN are ligands of FXR [71], yet our results suggest the flavonoids might also regulate FXR activity by modulating bile acid pool via activation of bile acid synthesis. In fact, through a mechanism that is still unclear, we and others [32, 41] have reported that XN, DXN and TXN, unlike FXR agonist CDCA, activate expression of CYP7A1, the rate-limiting enzyme in the conversion of cholesterol into BAs. The increase in hepatic primary unconjugated BAs in XN, DXN and TXN-treated mice associated with the reduction in hepatic cholesterol and the induction of CYP7A1 suggest a stimulation of *de novo* bile acid synthesis by the flavonoids. We did not observe a concomitant increase in total hepatic BAs, which can be partially explained by increased biliary excretion of BAs, as we previously reported that fecal excretion of BAs is increased in DXN- and TXN-treated mice [41]. BAs being signaling molecules with a central role in several physiopathological states, the modulation of bile acid profiles by the flavonoids is likely at the root of a cascade of signaling pathways, which would lead to the amelioration of metabolic function and neurocognitive impairment associated with obesity.

In summary, our results show that hops-derived flavonoids modulate the liver-brain axis, as improvement of peripheral and central metabolic impairments is linked to a decrease in ceramides in both the liver and hippocampus of treated mice. Moreover, XN, DXN and TXN promote *de novo* synthesis of BAs via CYP7A1 induction, revealing the flavonoids as modulators of bile acid composition. These data suggest that bile acid-mediated regulation of FXR activity might contribute to the amelioration of metabolic dysfunction through modulation of the bile acid-FXR-ceramide signaling axis in mice fed a HFD with XN, DXN or TXN. These findings are important as novel therapies targeting ceramide accumulation in brain and peripheral organs are promising approaches to alleviate obesity-related metabolic impairments.

Supplementary Material

Refer to Web version on PubMed Central for supplementary material.

Acknowledgements and grant support

The authors thank Yang Zhang for isolating the mRNA from mice liver samples. The National Institutes of Health (NIH grants 5R01AT009168, 1S10RR027878 and 3R01AT009168-04S1), the OSU College of Pharmacy, Hopsteiner, Inc. (New York) and the OSU Foundation Buhler-Wang Research Fund supported the research.

Abbreviations

BAs	bile acids
BSEP	bile salt export pump
CA	cholic acid
CE	cholesterol esters
Cer	ceramide
CERK	ceramide kinase
CERS	ceramide synthase
Chol	cholesterol
CYP7A1	cytochrome P450 Family 7 Subfamily A Member 1
DEGS	sphingolipid delta desaturase
DG	diglycerides
DXN	α,β-dihydroxanthohumol
FXR	Farnesoid X receptor
HDCA	hyodeoxycholic acid
HFD	high-fat diet
IS	Internal standard
IX	isoxanthohumol
KSR	3-keto sphinganine reductase
LPC	lysophosphatidylcholine
LPE	lysophosphatidylethanolamine
LPI	lysophosphatidylinositol
MCA	muricholic acid

MetS	metabolic syndrome
PC	phosphatidylcholine
PE	phosphatidylethanolamine
PI	phosphatidylinositol
PI3K	phosphoinositide-3-kinase
8PN	8-prenylnaringenin
PS	phosphatidylserine
SGMS	Sphingomyelin synthase
SHP	small heterodimer partner
SM	sphingomyelin
SMPD	sphingomyelin phosphodiesterase or sphingomyelinase
Spha	sphinganine
Spho	sphingosine
SPTLC	serine palmitoyl transferase
SREBP1c	Sterol regulatory element-binding protein 1c
TCA	taurocholic acid
TCDCA	taurochenodeoxycholic acid
TDCA	taurodeoxycholic acid
TG	triglycerides
T-MCA	tauromuricholic acid
TUDCA	tauroursodeoxycholic acid
TXN	tetrahydroxanthohumol
XN	xanthohumol

5. References

[1]. Shaw DI, Hall WL, Williams CM, Metabolic syndrome: what is it and what are the implications? Proceedings of the Nutrition Society 2005, 64, 349–357.

[2]. Grundy Scott M, Cleeman James I, Daniels Stephen R, Donato Karen A, Eckel Robert H, Franklin Barry A, Gordon David J, Krauss Ronald M, Savage Peter J, Smith Sidney C, Spertus John A, Costa F., Diagnosis and Management of the Metabolic Syndrome. Circulation 2005, 112, 2735–2752. [PubMed: 16157765]

[3]. Wong SK, Chin K-Y, Suhaimi FH, Fairus A, Ima-Nirwana S, Animal models of metabolic syndrome: a review. Nutrition & metabolism 2016, 13, 65–65. [PubMed: 27708685]

[4]. Pratchayasakul W, Kerdphoo S, Petsophonsakul P, Pongchaidecha A, Chattipakorn N, Chattipakorn SC., Effects of high-fat diet on insulin receptor function in rat hippocampus and the level of neuronal corticosterone. Life Sci 2011, 88, 619–627. [PubMed: 21315737]

[5]. Hariri N, Thibault L, High-fat diet-induced obesity in animal models. Nutr Res Rev 2010, 23, 270–299. [PubMed: 20977819]

[6]. Kahn SE, Hull RL, Utzschneider KM, Mechanisms linking obesity to insulin resistance and type 2 diabetes. Nature 2006, 444, 840–846. [PubMed: 17167471]

[7]. McTernan CL, McTernan PG, Harte AL, Levick PL, Barnett AH, Kumar S., Resistin, central obesity, and type 2 diabetes. The Lancet 2002, 359, 46–47.

[8]. Özcan U, Cao Q, Yilmaz E, Lee A-H, Iwakoshi NN, Özdelen E, Tuncman G, Görgün C, Glimcher LH, Hotamisligil GS., Endoplasmic Reticulum Stress Links Obesity, Insulin Action, and Type 2 Diabetes. Science 2004, 306, 457. [PubMed: 15486293]

[9]. Shulman GI, Cellular mechanisms of insulin resistance. The Journal of Clinical Investigation 2000, 106, 171–176. [PubMed: 10903330]

[10]. Summers SA, Garza LA, Zhou H, Birnbaum MJ, Regulation of Insulin-Stimulated Glucose Transporter GLUT4 Translocation and Akt Kinase Activity by Ceramide. Molecular and Cellular Biology 1998, 18, 5457. [PubMed: 9710629]

[11]. Pratchayasakul W, Sa-Nguanmoo P, Sivasinprasasn S, Pintana H, Tawinvisan R, Sripetchwandee J, Kumfu S, Chattipakorn N, Chattipakorn SC., Obesity accelerates cognitive decline by aggravating mitochondrial dysfunction, insulin resistance and synaptic dysfunction under estrogen-deprived conditions. Horm Behav 2015, 72, 68–77. [PubMed: 25989597]

[12]. Sa-Nguanmoo P, Tanajak P, Kerdphoo S, Satjaritanun P, Wang X, Liang G, Li X, Jiang C, Pratchayasakul W, Chattipakorn N, Chattipakorn SC., FGF21 improves cognition by restored synaptic plasticity, dendritic spine density, brain mitochondrial function and cell apoptosis in obese-insulin resistant male rats. Horm Behav 2016, 85, 86–95. [PubMed: 27566237]

[13]. Pipatpiboon N, Pratchayasakul W, Chattipakorn N, Chattipakorn SC, PPARgamma agonist improves neuronal insulin receptor function in hippocampus and brain mitochondria function in rats with insulin resistance induced by long term high-fat diets. Endocrinology 2012, 153, 329–338. [PubMed: 22109891]

[14]. Pintana H, Tanajak P, Pratchayasakul W, Sa-Nguanmoo P, Chunchai T, Satjaritanun P, Leelarphat L, Chattipakorn N, Chattipakorn SC., Energy restriction combined with dipeptidyl peptidase-4 inhibitor exerts neuroprotection in obese male rats. Br J Nutr 2016, 1–9.

[15]. Sripetchwandee J, Chattipakorn N, Chattipakorn SC, Links Between Obesity-Induced Brain Insulin Resistance, Brain Mitochondrial Dysfunction, and Dementia. Front Endocrinol (Lausanne) 2018, 9, 496. [PubMed: 30233495]

[16]. Holland WL, Brozinick JT, Wang L-P, Hawkins ED, Sargent KM, Liu Y, Narra K, Hoehn KL, Knotts TA, Siesky A, Nelson DH, Karathanasis SK, Greg K Fontenot MJ Birnbaum SA Summers., Inhibition of Ceramide Synthesis Ameliorates Glucocorticoid-, Saturated-Fat-, and Obesity-Induced Insulin Resistance. Cell Metabolism 2007, 5, 167–179. [PubMed: 17339025]

[17]. Merrill AH, De Novo Sphingolipid Biosynthesis: A Necessary, but Dangerous, Pathway. Journal of Biological Chemistry 2002, 277, 25843–25846.

[18]. Summers SA, Ceramides in insulin resistance and lipotoxicity. Progress in Lipid Research 2006, 45, 42–72. [PubMed: 16445986]

[19]. Bikman BT, Summers SA, Ceramides as modulators of cellular and whole-body metabolism. The Journal of Clinical Investigation 2011, 121, 4222–4230. [PubMed: 22045572]

[20]. Xie C, Jiang C, Shi J, Gao X, Sun D, Sun L, Wang T, Takahashi S, Anitha M, Krausz KW, Patterson AD, Gonzalez FJ., An Intestinal Farnesoid X Receptor–Ceramide Signaling Axis Modulates Hepatic Gluconeogenesis in Mice. Diabetes 2017, 66, 613. [PubMed: 28223344]

[21]. Zimmermann C, Ginis I, Furuya K, Klimanis D, Ruetzler C, Spatz M, Hallenbeck JM., Lipopolysaccharide-induced ischemic tolerance is associated with increased levels of ceramide in brain and in plasma. Brain Research 2001, 895, 59–65. [PubMed: 11259760]

[22]. Tong M, de la Monte SM, Mechanisms of ceramide-mediated neurodegeneration. J Alzheimers Dis 2009, 16, 705–714. [PubMed: 19387107]

[23]. Lyn-Cook LE Jr., Lawton M, Tong M, Silbermann E, Longato L, Jiao P, Mark P, Wands JR, Xu H, de la Monte SM., Hepatic ceramide may mediate brain insulin resistance and neurodegeneration in type 2 diabetes and non-alcoholic steatohepatitis. J Alzheimers Dis 2009, 16, 715–729. [PubMed: 19387108]

[24]. Turpin Sarah M., Nicholls Hayley T., Willmes Diana M., Mourier A, Brodesser S, Wunderlich Claudia M., Mauer J, Xu E, Hammerschmidt P, Brönneke Hella S., Trifunovic A, LoSasso G, Wunderlich FT, Kornfeld J-W, Blüher M, Krönke M, Brüning. Jens C., Obesity-Induced CerS6-Dependent C16:0 Ceramide Production Promotes Weight Gain and Glucose Intolerance. Cell Metabolism 2014, 20, 678–686. [PubMed: 25295788]

[25]. Jiang C, Xie C, Lv Y, Li J, Krausz KW, Shi J, Brocker CN, Desai D, Amin SG, Bisson WH, Liu Y, Gavrilova O, Patterson AD, Gonzalez FJ., Intestine-selective farnesoid X receptor inhibition improves obesity-related metabolic dysfunction. Nature Communications 2015, 6, 10166.

[26]. Shapiro H, Kolodziejczyk AA, Halstuch D, Elinav E, Bile acids in glucose metabolism in health and disease. The Journal of Experimental Medicine 2018, 215, 383. [PubMed: 29339445]

[27]. Brandvold KR, Weaver JM, Whidbey C, Wright AT, A continuous fluorescence assay for simple quantification of bile salt hydrolase activity in the gut microbiome. Scientific Reports 2019, 9, 1359. [PubMed: 30718677]

[28]. Joyce SA, MacSharry J, Casey PG, Kinsella M, Murphy EF, Shanahan F, Hill C, Gahan CGM., Regulation of host weight gain and lipid metabolism by bacterial bile acid modification in the gut. Proceedings of the National Academy of Sciences 2014, 111, 7421.

[29]. Makishima M, Lu TT, Xie W, Whitfield GK, Domoto H, Evans RM, Haussler MR, Mangelsdorf DJ., Vitamin D receptor as an intestinal bile acid sensor. Science 2002, 296, 1313–1316. [PubMed: 12016314]

[30]. Kawamata Y, Fujii R, Hosoya M, Harada M, Yoshida H, Miwa M, Fukusumi S, Habata Y, Itoh T, Shintani Y, Hinuma S, Fujisawa Y, Fujino M., A G protein-coupled receptor responsive to bile acids. J Biol Chem 2003, 278, 9435–9440. [PubMed: 12524422]

[31]. Legette LL, Moreno Luna AY, Reed RL, Miranda CL, Bobe G, Proteau RR, Stevens JF., Xanthohumol lowers body weight and fasting plasma glucose in obese male Zucker fa/fa rats. Phytochemistry 2013, 91, 236–241. [PubMed: 22640929]

[32]. Nozawa H, Xanthohumol, the chalcone from beer hops (Humulus lupulus L.), is the ligand for farnesoid X receptor and ameliorates lipid and glucose metabolism in KK-A(y) mice. Biochem Biophys Res Commun 2005, 336, 754–761. [PubMed: 16140264]

[33]. Miranda CL, Elias VD, Hay JJ, Choi J, Reed RL, Stevens JF., Xanthohumol improves dysfunctional glucose and lipid metabolism in diet-induced obese C57BL/6J mice. Arch Biochem Biophys 2016, 599, 22–30. [PubMed: 26976708]

[34]. Miranda CL, Johnson LA, de Montgolfier O, Elias VD, Ullrich LS, Hay JJ, Paraiso IL, Choi J, Reed RL, Revel JS, Kioussi C, Bobe G, Iwaniec UT, Turner RT, Katzenellenbogen BS, Katzenellenbogen JA, Blakemore PR, Gombart AF, Maier CS, Raber J, Stevens JF., Non-estrogenic Xanthohumol Derivatives Mitigate Insulin Resistance and Cognitive Impairment in High-Fat Diet-induced Obese Mice. Sci Rep 2018, 8, 613. [PubMed: 29330372]

[35]. Possemiers S, Bolca S, Grootaert C, Heyerick A, Decroos K, Dhooge W, De Keukeleire D, Rabot S, Verstraete W, Van de Wiele T., The Prenylflavonoid Isoxanthohumol from Hops (Humulus lupulus L.) Is Activated into the Potent Phytoestrogen 8-Prenylnaringenin In Vitro and in the Human Intestine. The Journal of Nutrition 2006, 136, 1862–1867. [PubMed: 16772450]

[36]. Guo J, Nikolic D, Chadwick LR, Pauli GF, van Breemen RB, Identification of human hepatic cytochrome P450 enzymes involved in the metabolism of 8-prenylnaringenin and isoxanthohumol from hops (Humulus lupulus L.). Drug Metab Dispos 2006, 34, 1152–1159. [PubMed: 16611861]

[37]. Costa R, Rodrigues I, Guardão L, Rocha-Rodrigues S, Silva C, Magalhães J, Ferreira-de-Almeida M, Negrão R, Soares R., Xanthohumol and 8-prenylnaringenin ameliorate diabetic-related metabolic dysfunctions in mice. The Journal of Nutritional Biochemistry 2017, 45, 39–47. [PubMed: 28431322]

[38]. Paraiso IL, Plagmann LS, Yang L, Zielke R, Gombart AF, Maier CS, Sikora AE, Blakemore PR, Stevens JF., Reductive Metabolism of Xanthohumol and 8-Prenylnaringenin by the Intestinal Bacterium Eubacterium ramulus. Mol Nutr Food Res 2019, 63, e1800923. [PubMed: 30471194]

[39]. McDougall MQ, Choi J, Stevens JF, Truong L, Tanguay RL, Traber MG., Lipidomics and H218O labeling techniques reveal increased remodeling of DHA-containing membrane phospholipids associated with abnormal locomotor responses in α-tocopherol deficient zebrafish (danio rerio) embryos. Redox Biology 2016, 8, 165–174. [PubMed: 26774753]

[40]. Choi J, Leonard SW, Kasper K, McDougall M, Stevens JF, Tanguay RL, Traber MG., Novel function of vitamin E in regulation of zebrafish (Danio rerio) brain lysophospholipids discovered using lipidomics. Journal of Lipid Research 2015, 56, 1182–1190. [PubMed: 25855633]

[41]. Zhang Y, Bobe G, Revel JS, Rodrigues RR, Sharpton TJ, Fantacone ML, Raslan K, Miranda CL, Lowry MB, Blakemore PR, Morgun A, Shulzhenko N, Maier CS, Stevens JF, Gombart AF., Improvements in Metabolic Syndrome by Xanthohumol Derivatives Are Linked to Altered Gut Microbiota and Bile Acid Metabolism. Mol Nutr Food Res 2019, e1900789. [PubMed: 31755244]

[42]. Liu B, Obeid LM, Hannun YA, Sphingomyelinases in cell regulation. Seminars in Cell & Developmental Biology 1997, 8, 311–322. [PubMed: 10024495]

[43]. Shah C, Yang G, Lee I, Bielawski J, Hannun YA, Samad F., Protection from high fat diet-induced increase in ceramide in mice lacking plasminogen activator inhibitor 1. J Biol Chem 2008, 283, 13538–13548. [PubMed: 18359942]

[44]. Reynolds CP, Maurer BJ, Kolesnick RN, Ceramide synthesis and metabolism as a target for cancer therapy. Cancer Letters 2004, 206, 169–180. [PubMed: 15013522]

[45]. Ong JP, Younossi ZM, Epidemiology and Natural History of NAFLD and NASH. Clinics in Liver Disease 2007, 11, 1–16. [PubMed: 17544968]

[46]. Puri P, Baillie RA, Wiest MM, Mirshahi F, Choudhury J, Cheung O, Sargeant C, Contos MJ, Sanyal AJ., A lipidomic analysis of nonalcoholic fatty liver disease. Hepatology 2007, 46, 1081–1090. [PubMed: 17654743]

[47]. Mahli A, Seitz T, Freese K, Frank J, Weiskirchen R, Abdel-Tawab M, Behnam D, and Hellerbrand C, Therapeutic Application of Micellar Solubilized Xanthohumol in a Western-Type Diet-Induced Mouse Model of Obesity, Diabetes and Non-Alcoholic Fatty Liver Disease. Cells 2019, 8.

[48]. Tabata N, Ito M, Tomoda H, Omura S, Xanthohumols, diacylglycerol acyltransferase inhibitors, from Humulus lupulus. Phytochemistry 1997, 46, 683–687. [PubMed: 9366096]

[49]. Yu XX, Murray SF, Pandey SK, Booten SL, Bao D, Song X-Z, Kelly S, Chen S, McKay R, Monia BP, Bhanot S., Antisense oligonucleotide reduction of DGAT2 expression improves hepatic steatosis and hyperlipidemia in obese mice. Hepatology 2005, 42, 362–371. [PubMed: 16001399]

[50]. Smith SJ, Cases S, Jensen DR, Chen HC, Sande E, Tow B, Sanan DA, Raber J, Eckel RH, Farese RV., Obesity resistance and multiple mechanisms of triglyceride synthesis in mice lacking Dgat. Nature Genetics 2000, 25, 87–90. [PubMed: 10802663]

[51]. Cantero I, Abete I, del Bas JM, Caimari A, Arola L, Zulet MA, Martinez JA., Changes in lysophospholipids and liver status after weight loss: the RESMENA study. Nutrition & Metabolism 2018, 15, 51. [PubMed: 30026784]

[52]. Graessler J, Schwudke D, Schwarz PE, Herzog R, Shevchenko A, Bornstein SR., Top-down lipidomics reveals ether lipid deficiency in blood plasma of hypertensive patients. PLoS One 2009, 4, e6261. [PubMed: 19603071]

[53]. Pietilainen KH, Sysi-Aho M, Rissanen A, Seppanen-Laakso T, Yki-Jarvinen H, Kaprio J, Oresic M., Acquired obesity is associated with changes in the serum lipidomic profile independent of genetic effects--a monozygotic twin study. PLoS One 2007, 2, e218. [PubMed: 17299598]

[54]. Kim H-J, Kim JH, Noh S, Hur HJ, Sung MJ, Hwang J-T, Park JH, Yang HJ, Kim M-S, Kwon DY, Yoon SH., Metabolomic Analysis of Livers and Serum from High-Fat Diet Induced Obese Mice. Journal of Proteome Research 2011, 10, 722–731. [PubMed: 21047143]

[55]. Rauschert S, Uhl O, Koletzko B, Kirchberg F, Mori TA, Huang R-C, Beilin LJ, Hellmuth C, Oddy WH., Lipidomics Reveals Associations of Phospholipids With Obesity and Insulin Resistance in Young Adults. The Journal of Clinical Endocrinology & Metabolism 2016, 101, 871–879. [PubMed: 26709969]

[56]. Hernández-Alvarez MI, Sebastián D, Vives S, Ivanova S, Bartoccioni P, Kakimoto P, Plana N, Veiga SR, Hernández V, Vasconcelos N, Peddinti G, Adrover A, Jové M, Pamplona R, Gordaliza-Alaguero I, Calvo E, Cabré N, Castro R, Kuzmanic A, Boutant M, Sala D, Hyotylainen T, Orešič M, Fort J, Errasti-Murugarren E, Rodrígues CMP, Orozco M, Joven J, Cantó C, Palacin M, Fernández-Veledo S, Vendrell J, Zorzano A., Deficient Endoplasmic Reticulum-Mitochondrial Phosphatidylserine Transfer Causes Liver Disease. Cell 2019, 177, 881–895.e817. [PubMed: 31051106]

[57]. Kim H-Y, Huang BX, Spector AA, Phosphatidylserine in the brain: Metabolism and function. Progress in Lipid Research 2014, 56, 1–18. [PubMed: 24992464]

[58]. de la Monte SM, Tong M, Nguyen V, Setshedi M, Longato L, Wands JR, Ceramide-mediated insulin resistance and impairment of cognitive-motor functions. J Alzheimers Dis 2010, 21, 967–984. [PubMed: 20693650]

[59]. Arboleda G, Huang TJ, Waters C, Verkhratsky A, Fernyhough P, Gibson RM., Insulin-like growth factor-1-dependent maintenance of neuronal metabolism through the phosphatidylinositol 3-kinase-Akt pathway is inhibited by C2-ceramide in CAD cells. Eur J Neurosci 2007, 25, 3030–3038. [PubMed: 17561816]

[60]. Arboleda G, Morales LC, Benitez B, Arboleda H, Regulation of ceramide-induced neuronal death: cell metabolism meets neurodegeneration. Brain Res Rev 2009, 59, 333–346. [PubMed: 18996148]

[61]. Tu J, Yin Y, Xu M, Wang R, Zhu Z-J, Absolute quantitative lipidomics reveals lipidome-wide alterations in aging brain. Metabolomics 2017, 14, 5. [PubMed: 30830317]

[62]. Giusto NM, Roque ME, Ilincheta de Boschero MG, Effects of aging on the content, composition and synthesis of sphingomyelin in the central nervous system. Lipids 1992, 27, 835–839. [PubMed: 1491598]

[63]. Degirolamo C, Modica S, Palasciano G, Moschetta A, Bile acids and colon cancer: Solving the puzzle with nuclear receptors. Trends in Molecular Medicine 2011, 17, 564–572. [PubMed: 21724466]

[64]. Chiang JYL, Bile acids: regulation of synthesis. Journal of lipid research 2009, 50, 1955–1966. [PubMed: 19346330]

[65]. Han CY, Update on FXR Biology: Promising Therapeutic Target? International journal of molecular sciences 2018, 19, 2069.

[66]. Jiang C, Xie C, Li F, Zhang L, Nichols RG, Krausz KW, Cai J, Qi Y, Fang Z-Z, Takahashi S, Tanaka N, Desai D, Amin SG, Albert I, Patterson AD, Gonzalez FJ., Intestinal farnesoid X receptor signaling promotes nonalcoholic fatty liver disease. The Journal of Clinical Investigation 2015, 125, 386–402. [PubMed: 25500885]

[67]. Xia Y, Zhang F, Zhao S, Li Y, Chen X, Gao E, Xu X, Xiong Z, Zhang X, Zhang J, Zhao H, Wang W, Wang H, Guo Y, Liu Y, Li C, Wang S, Zhang L, Yan W, Tao L., Adiponectin determines farnesoid X receptor agonism-mediated cardioprotection against post-infarction remodelling and dysfunction. Cardiovascular Research 2018, 114, 1335–1349. [PubMed: 29668847]

[68]. Xin X, Zhong M, Zhang S, Peng Y, Zhu W, Zhang Y., [Effects of farnesoid X receptor agonist on adiponectin and its receptors]. Nan Fang Yi Ke Da Xue Xue Bao 2014, 34, 109–112. [PubMed: 24463129]

[69]. Holland WL, Miller RA, Wang ZV, Sun K, Barth BM, Bui HH, Davis KE, Bikman BT, Halberg N, Rutkowski JM, Wade MR, Tenorio VM, Kuo M-S, Brozinick JT, Zhang BB, Birnbaum MJ, Summers SA, Scherer PE., Receptor-mediated activation of ceramidase activity initiates the pleiotropic actions of adiponectin. Nature Medicine 2010, 17, 55.

[70]. Miyata S, Inoue J, Shimizu M, Sato R, Xanthohumol Improves Diet-induced Obesity and Fatty Liver by Suppressing Sterol Regulatory Element-binding Protein (SREBP) Activation. Journal of Biological Chemistry 2015, 290, 20565–20579.

[71]. Yang L, Broderick D, Campbell Y, Gombart AF, Stevens JF, Jiang Y, Hsu VL, Bisson WH, Maier CS., Conformational modulation of the farnesoid X receptor by prenylflavonoids: Insights from hydrogen deuterium exchange mass spectrometry (HDX-MS), fluorescence titration and molecular docking studies. Biochim Biophys Acta 2016, 1864, 1667–1677. [PubMed: 27596062]

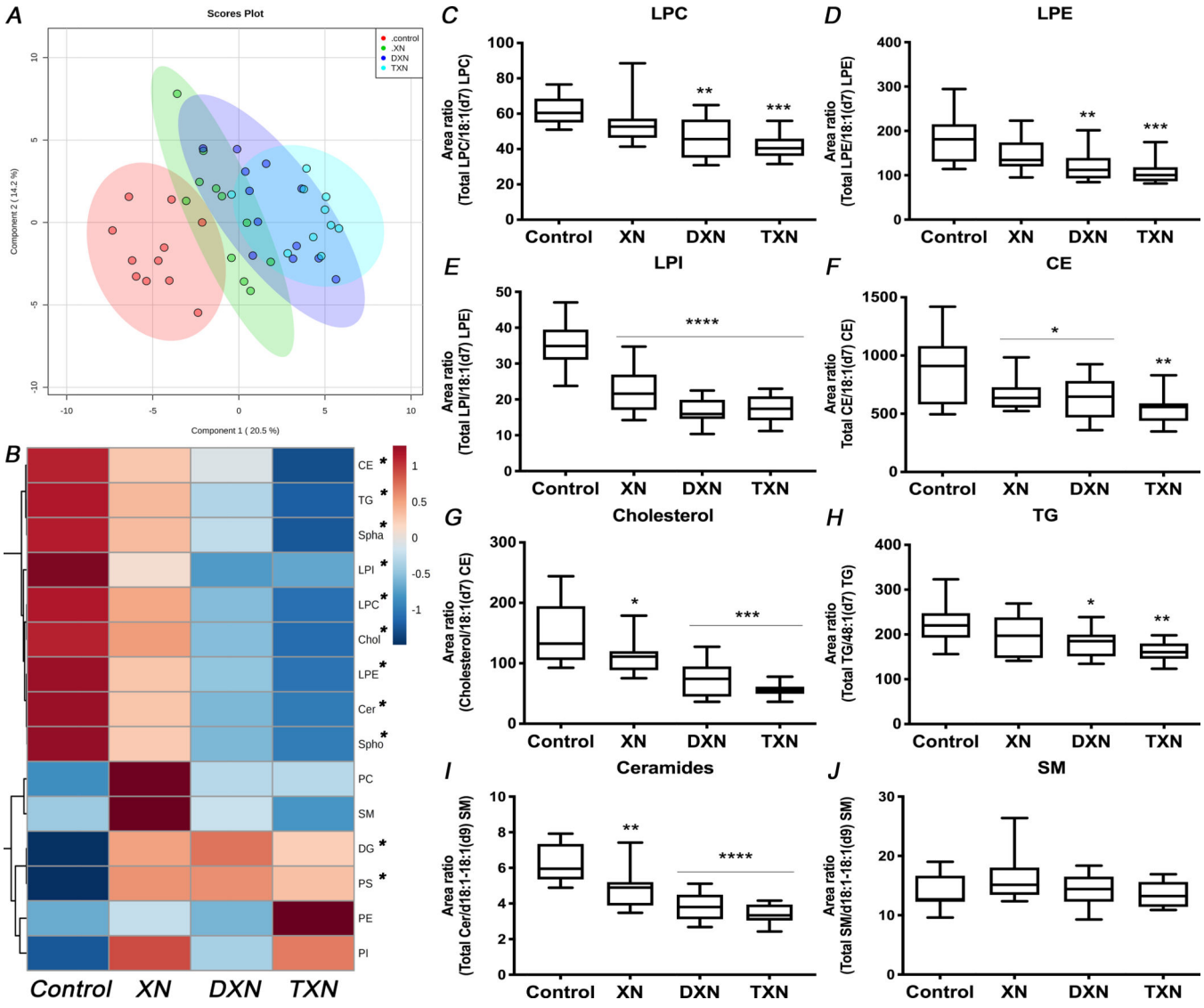

Fig. 1. XN, DXN and TXN modify hepatic lipid profiles in HFD-fed mice.

(A) Partial least-squares discriminant analysis (PLS-DA) modeling of 148 hepatic lipids in control and treatment groups. (B) Heatmap of different lipid sub-classes according to hierarchical clustering in control and treatment groups. (C-E) Hepatic lysophospholipids, (F) cholesterol esters, (G) cholesterol, (H) TG, (I) ceramides and (J) SM relative abundance (n = 9–12 per group). *p < 0.05, **p < 0.01, ***p < 0.001, ****p < 0.0001.

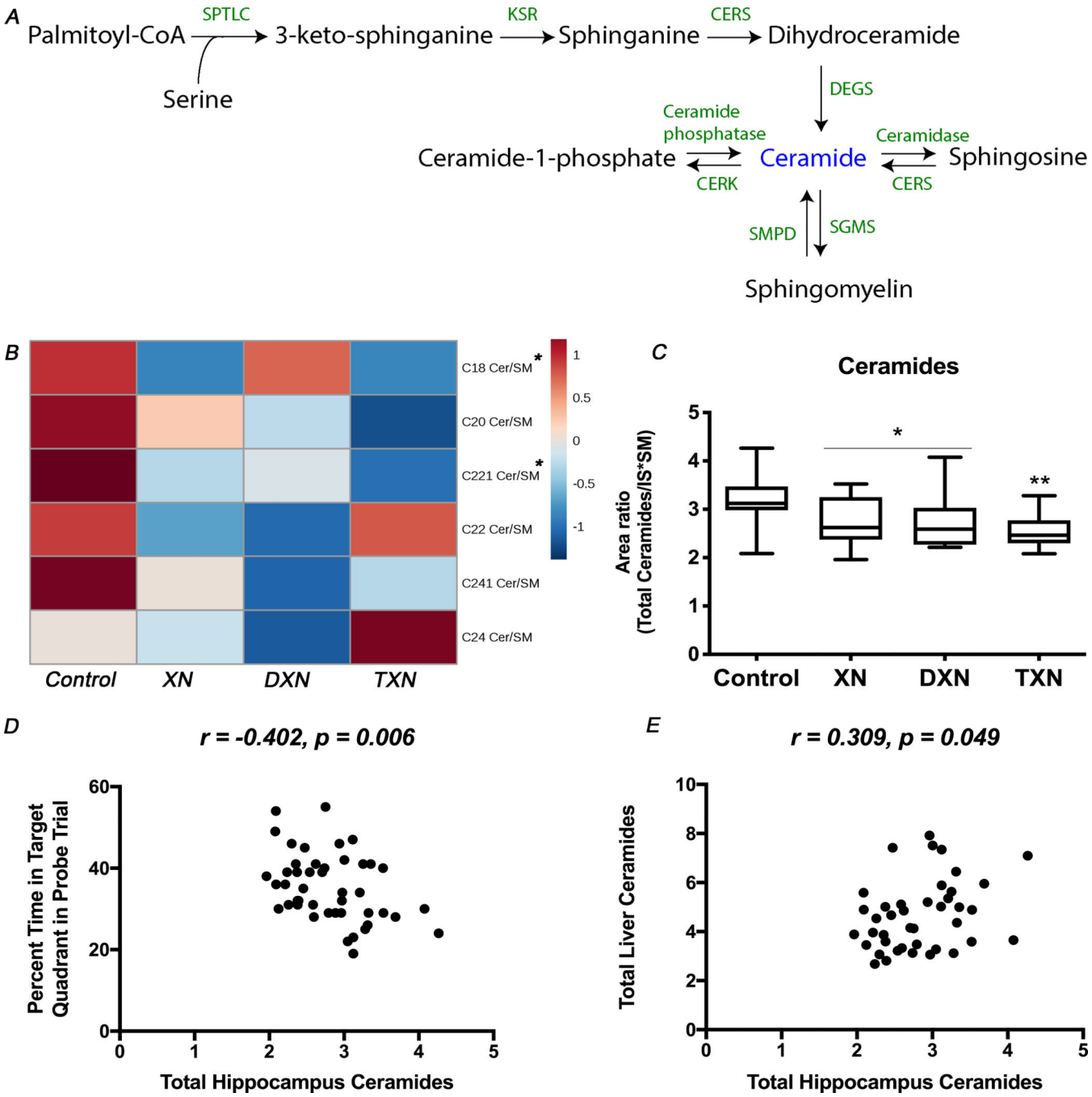

Fig. 2. XN, DXN and TXN decrease hippocampal ceramides in HFD-fed mice.

(A) Ceramide metabolism in mammalian cells: ceramides can be synthesized *de novo* from fatty acids or sphingosines through the actions of serine palmitoyl transferase and ceramide synthases, which starts on the cytoplasmic face of the endoplasmic reticulum. Ceramides can also be generated from SM catabolism by sphingomyelinases or through degradation of complex sphingolipids in late endosomes and lysosomes. (B) Heatmap of annotated ceramide species in the hippocampus of control and treated mice. (C) Total amounts of ceramides in the hippocampus of control and treated mice (n = 9–12 per group). (D)

Correlation between relative abundance of ceramides in the hippocampus and percent time in the target quadrant during the probe trial ($r = -0.402$, $p = 0.006$, $n = 45$ data points). (E) Correlation between relative abundance of ceramides in the hippocampus and in the liver ($r = 0.309$, $p = 0.049$, $n = 41$ data points). *p < 0.05, **p < 0.01.

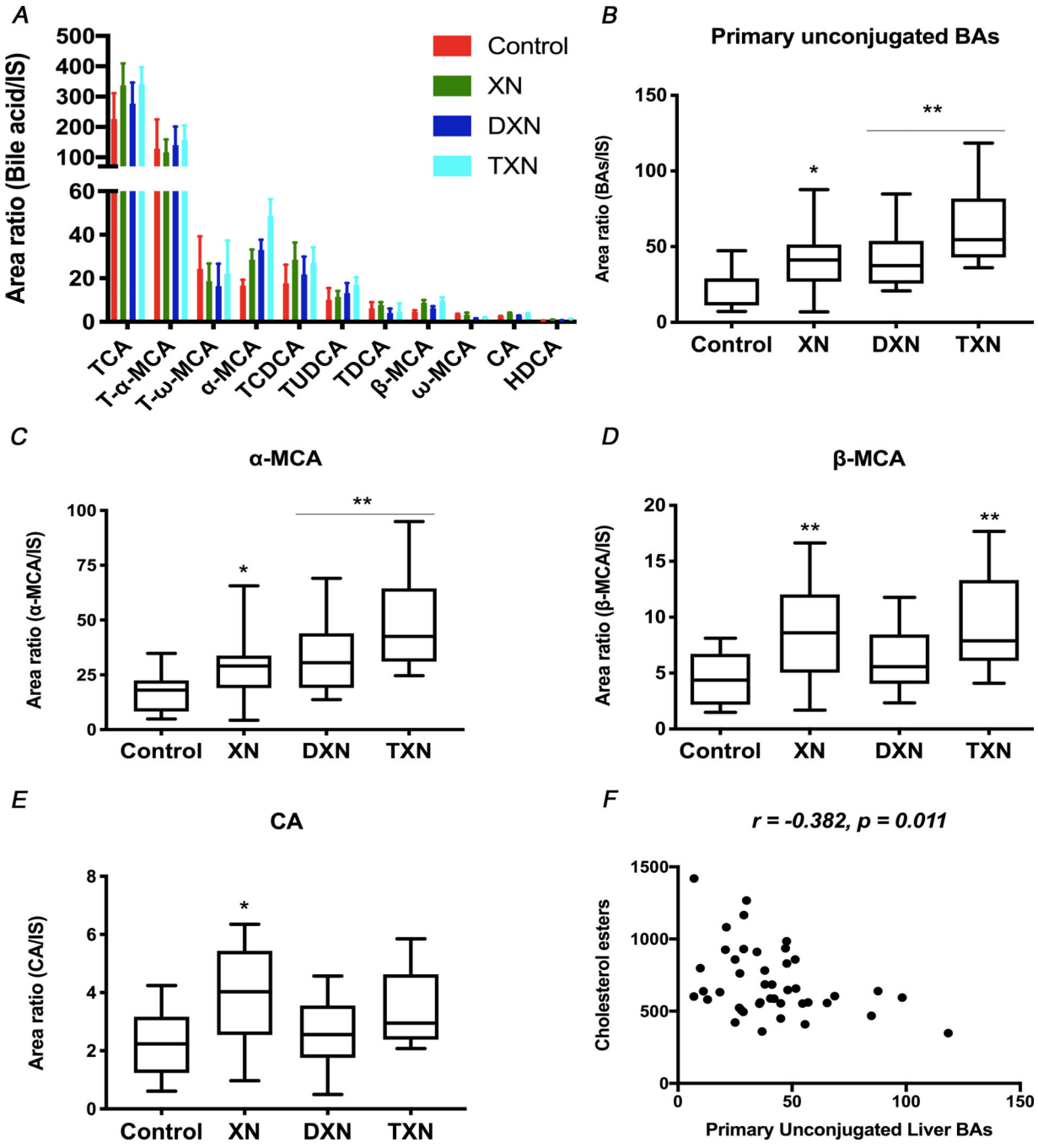

Fig. 3. XN, DXN and TXN modify hepatic bile acid profiles in HFD-fed mice.

Relative abundance of (A) Annotated bile acids, (B) Primary unconjugated bile acids, (C) α-MCA, (D) β-MCA, and (E) CA measured by UPLC-MS in the liver of control and treated mice (n = 9–12 per group). (F) Correlation between primary unconjugated bile acids and cholesterol esters in the liver ($r = -0.365$, $p = 0.018$, $n = 43$ data points). *p < 0.05, **p < 0.01, ***p < 0.001.

Table 1.

Dietary XN and its hydrogenated derivatives DXN and TXN affect in different ways expression of genes involved in ceramide anabolism and catabolism in the liver of HFD-fed mice. Data are shown as Log_2 Fold Change Treated/Control ± SEM of n = 4–5 per group. HFD-fed mice were used as reference.

	XN-treated mice	DXN-treated mice	TXN-treated mice
Sptlc1	0.40 ± 0.22	0.63 * ± 0.22	0.78 ** ± 0.22
Sptlc2	0.04 ± 0.25	0.17 ± 0.25	−0.003 ± 0.25
Degs1	0.21 ± 0.22	−0.02 ± 0.22	0.29 ± 0.22
Degs2	0.64 * ± 0.27	0.14 ± 0.27	0.21 ± 0.27
Cers2	0.60 * ± 0.22	0.18 ± 0.22	−0.10 ± 0.22
Cers4	0.91 ** ± 0.23	0.05 ± 0.23	0.10 ± 0.23
Cers5	1.65 *** ± 0.32	0.44 ± 0.28	0.48 ± 0.28
Cers6	0.81 * ± 0.21	0.16 ± 0.21	0.11 ± 0.21
Smpd1	0.88 * ± 0.30	0.36 ± 0.30	0.47 ± 0.30
Smpd3	1.02 * ± 0.42	−0.63 ± 0.42	−0.82 ± 0.38
Smpd4	1.45 *** ± 0.27	0.82 ** ± 0.27	0.63 * ± 0.27
Sgms1	1.14 * ± 0.42	−0.24 ± 0.38	−0.23 ± 0.38
Sgms2	0.87 ** ± 0.28	−0.25 ± 0.28	−0.07 ± 0.28

* $p < 0.05$

** $p < 0.01$

*** $p < 0.001$

**** $p < 0.0001$.

Table 2.

XN, DXN and TXN induce expression of FXR target genes in HepG2 cell lines, their effect is stronger than FXR agonist CDCA. Data are shown as Log_2 Fold Change Treated/Control ± SEM of n = 3 per group. Vehicle-treated cells were used as reference.

	CDCA	XN	DXN	TXN
Shp	0.93** ± 0.27	1.21** ± 0.27	1.92**** ± 0.27	1.474*** ± 0.27
Cyp7a1	−0.26 ± 0.29	4.29**** ± 0.29	2.34**** ± 0.29	1.13** ± 0.29
Bsep	−0.02 ± 0.25	1.21** ± 0.25	2.41**** ± 0.25	0.60* ± 0.25
Srebp1c	−0.50 ± 0.24	−0.31 ± 0.24	0.39 ± 0.24	0.64* ± 0.24

* $p < 0.05$

** $p < 0.01$

*** $p < 0.001$

**** $p < 0.0001$.